GEOLOGICA CARPATHICA, JUNE 2013, 64, 3, 171–180 doi: 10.2478/geoca-2013-0018

Gallium and germanium geochemistry during magmatic fractionation and post-magmatic alteration in different types of granitoids: a case study from the Bohemian Massif (Czech Republic)

KAREL BREITER[1], NINA GARDENOVÁ[2], VIKTOR KANICKÝ[2] and TOMÁŠ VACULOVIČ[3]

[1]Institute of Geology, Academy of Sciences of the Czech Republic, v.v.i., Rozvojová 269, CZ-165 00 Praha 6-Lysolaje, Czech Republic; breiter@gli.cas.cz
[2]Faculty of Science, Masaryk University, Kotlářská 2, CZ-611 37 Brno, Czech Republic
[3]CEITEC, Masaryk University, Kamenice 5, CZ-625 00 Brno, Czech Republic

(Manuscript received October 19, 2012; accepted in revised form March 14, 2013)

Abstract: Contents of Ga and Ge in granites, rhyolites, orthogneisses and greisens of different geochemical types from the Bohemian Massif were studied using inductively coupled plasma mass spectrometry analysis of typical whole-rock samples. The contents of both elements generally increase during fractionation of granitic melts: Ga from 16 to 77 ppm and Ge from 1 to 5 ppm. The differences in Ge and Ga contents between strongly peraluminous (S-type) and slightly peraluminous (A-type) granites were negligible. The elemental ratios of Si/1000Ge and Al/1000Ga significantly decreased during magmatic fraction: from ca. 320 to 62 and from 4.6 to 1.2, respectively. During greisenization, Ge is enriched and hosted in newly formed hydrothermal topaz, while Ga is dispersed into fluid. The graph Al/Ga vs. Y/Ho seems to be useful tool for geochemical interpretation of highly evolved granitoids.

Key words: ICP-MS, geochemistry, granites, gallium, germanium.

Introduction

Gallium and germanium are relatively scarce elements and have chemical characteristics similar to those of the common elements Al and Si, respectively. Minerals with substantial amounts of Ga and Ge are rare. Gallium forms only several rare species such as gallite ($CuGaS_2$) and sohngeite ($Ga(OH)_3$). Germanium forms about 25 rare species, such as germanite ($Cu_{26}Fe_4Ge_4S_{32}$), renierite ($(Cu,Zn)_{11}(Ge,As)_2Fe_4S_{16}$), argyrodite ($Ag_8GeS_6$), and argutite ($GeO_2$). Generally, Ga and Ge are disseminated in rocks in minerals of Al and Si (camouflage principle for trace element distribution according to Goldschmidt 1937), which makes these two elements suitable geochemical tracers of past geological processes.

The known whole-rock and mineral abundances of Ga and Ge up to1970 were summarized by Wedepohl (1972), and data for Ge through 2006 were published by Höll et al. (2007). The reason for the little interest of petrologists in Ga and Ge lies in the difficulty involved in chemically identifying both elements because their contents cannot be established using conventional analytical methods such as X-ray fluorescence (XRF), atomic absorption spectrometry (AAS) or inductively coupled plasma with optical emission spectrometry. Nevertheless, Ga has recently been determined (using namely the ICP-MS technique) in bulk-rock samples more frequently than Ge (e.g. Goodman 1972; Argollo & Schilling 1978; Collins et al. 1982; Whalen et al. 1987; Paktunc & Cabri 1995; Macdonald et al. 2007, 2010; Flude et al. 2008; Kelly et al. 2008). Selected published whole-rock data of Ga and Ge are summarized in Table 1.

The relative behaviour of pairs of chemical elements with similar geochemical properties has been studied for many years. Pairs of chemical elements with identical valence bonds but different deeper electron structures behave in similar manners both chemically and geochemically (Goldschmidt 1937; Clarke 1992; Best 2003; Shaw 2006). They have similar ionic radii and ionization potentials. Particularly important is the fact, that proportions of such pairs of chemical elements are independent of their absolute abundances. Different properties of the deeper atomic structure, which may induce change in element proportions, are manifested only in specific condi-

Table 1: Published contents of Ga and Ge in magmatic rocks (ppm).

Material	Source	Ga	Ge
Earth	Webelement*	19	1.4
Chondrite	Anders & Grevesse (1989)	10	33
Oceanic bazalt	Paktunc & Cabri (1995)	14–25	
Granites	Collins et al. (1982)	12–22	
I-type granites	Whalen et al. (1987)	16±2	
S-type granites	Whalen et al. (1987)	17±2	
A-type granites	Whalen et al. (1987)	24.6±6	
Rhyolite, granite	Shaw (1957)	16	
Tonalite, granodiorite	Shaw (1957)	21.4	
Alkaline rhyolite	Macdonald et al. (2010)	29–33	
Hawaiian bazalt	Argollo & Schilling (1978)	18–27	1.1–1.5
Granites	Wedepohl et al. (1972)	15–35	1–3
Alkaline rocks	Wedepohl et al. (1972)	20–76	1–3
Rhyolitic glases	Macdonald et al. (2007)		2.2–3.9
Granites	Bernstein (1985)		0.5–4.0

* — www.webelements.com

tions. This means that an unusual elemental ratio in a particular rock sample can provide information about specific processes that occurred during the evolution of the rock.

Pairs of chemical elements, such as K-Rb, Nb-Ta or Zr-Hf, have been studied because they play an essential role in petrology and mineralogy (Černý et al. 1986; Clarke 1992; Linnen & Kepler 1997; Uher et al. 1998; Finch & Hanchar 2003; Hoskin & Schaltegger 2003; Breiter et al. 2006, 2007b). They reflect the evolution of silicate melts through fractional crystallization or fluid-melt immiscibility. In theory, Al-Ga and Si-Ge pairs may play a similar role in petrological interpretations. However, in practice these pairs have been utilized only sporadically. The existing petrological studies of the behaviour of Ga and Ge during fractionation of silicate melts have focused almost exclusively on volcanic rocks: Paktunc & Cabri (1995) compiled data for Ga in oceanic basalts ranging from 15 to 25 ppm. Argollo & Schilling (1978) studied Si/Ge and Al/Ga ratios in Hawaiian basalts. Macdonald et al. (2007, 2010) found 2.3–3.9 ppm Ge and 28.9–33.3 ppm Ga in glassy matrix from peralkaline rhyolites from the Kenya Rift Valley. The Al/Ga and Si/Ge ratios in aforementioned rocks range between 1,000–10,000 and 100,000–1,000,000, respectively.

In the field of granitoids, Collins et al. (1982) and Whalen et al. (1987) analysed 163 samples of different granitoids containing 15–50 ppm Ga and proposed to use the Ga/Al ratio for geochemical discrimination of A-type granites (10000Ga/Al > 2.6, i.e. Al/Ga < 3800 in A-type granites). According to Cotton & Wilkinson (1980), GaF_6^{3+} complexes are more stable in water-undersaturated melts than AlF_6^{3+}; this may be the reason for the increase in Ga/Al ratios in A-type melts.

In the case of Ge, no models of its behaviour in magmatic processes have been proposed. Wedepohl (1972) summarized the Ge contents of granitoids from 1 to 3 ppm. Some older studies stressed the enrichment of Ge during the greisenization of granites (Shcherba et al. 1966).

The aims of this paper, based on samples from the Bohemian Massif, are: (1) to provide pilot data on contents of Ga and Ge in granitoids of different geochemical types; (2) to discuss the changes in Al/Ga and Si/Ge ratios as a result of (i) different magma protoliths and (ii) different degrees of fractionation; (3) to assess the possibility of using Al/Ga and Si/Ge ratios for petrological considerations and interpretations.

Geological setting and studied samples

Within the Bohemian Massif, several contrasting types of Paleozoic granitoid plutons (Cháb et al. 2010) occur. The complexes of granitic rocks (plutons) selected for this study include the major types of magmas intruding during the Late Cambrian and Carboniferous in Central Europe. Some of the plutons comprise suites of intrusions that differ in their degrees of fractionation, for example, in their contents of major and trace elements. Therefore, the samples studied here combine the differences resulting from the parent magma composition, with differences caused by melt fractionation and other possible mechanisms. The following main types of Paleozoic granitoid plutons in the Bohemian Massif were collected (Fig. 1, Table 2):

The Cambro-Ordovician peraluminous intrusive complex in the Moldanubicum, which has been transformed into ortho-

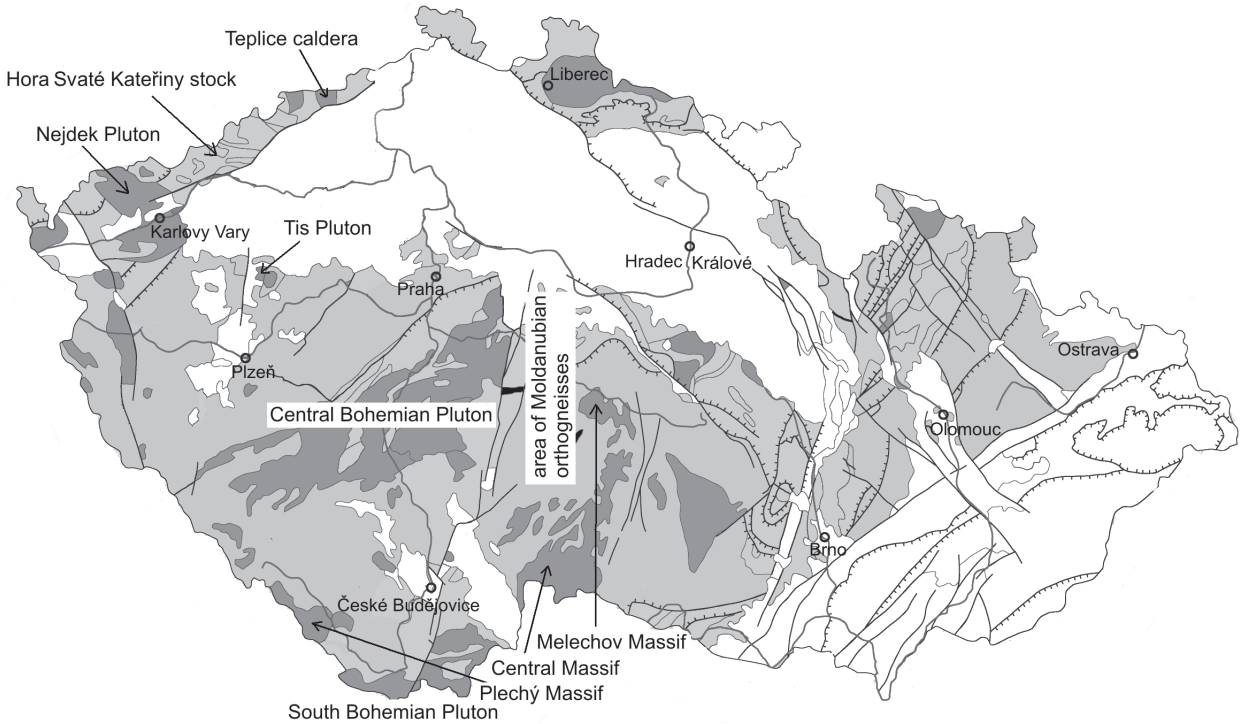

Fig. 1. Distribution of the studied granitic plutons within the Bohemian Massif, Czech Republic (from Cháb et al. 2010, modified). Black — orthogneiss, dark grey — granitoids, light grey — Variscan basement, white — post-Variscan sedimentary cover.

Table 2: List of samples with contents of Si, Al, Ge and Ga including standard deviations (samples are ordered according to their approximate grade of differentiation within individual plutons or massifs). *Continued on the next page.*

No.	Locality	Description	SiO_2	Al_2O_3	Ge	Ga
Moldanubicum orthogneisses, S-type			**wt. % (SD)**	**wt. % (SD)**	**ppm (SD)**	**ppm (SD)**
4080	Želiv, outcrop	Biotite orthogneiss	70.1 (0.4)	15.8 (0.3)	1.3 (0.1)	22.6 (0.4)
4069	Cetoraz, outcrop	Biotite orthogneiss	70.8 (0.4)	15.0 (0.2)	1.7 (0.1)	18.3 (0.7)
4066	Psárov, outcrop	Biotite orthogneiss	70.5 (0.5)	14.8 (0.2)	1.7 (0.2)	19.8 (0.9)
4072	Šelenberk near Mladá Vožice, outcrop	Biotite-muscovite orthogneiss	72.9 (0.3)	13.5 (0.1)	1.6 (0.1)	19.8 (0.4)
4074	Velký Blaník hill, outcrop	Biotite-muscovite orthogneiss	72.9 (0.6)	14.6 (0.3)	3.2 (0.3)	21 (1)
3266	Březí near Čáslav, outcrop	Biotite-muscovite orthogneiss	74.0 (0.5)	14.5 (0.2)	2.7 (0.3)	20.9 (0.5)
3796	Keblov, outcrop	Muscovite-tourmaline-biotite orthogneiss	72.8 (0.8)	14.6 (0.3)	2.7 (0.2)	19.1 (0.8)
3262	Quarry Přibyslavice near Čáslav	Muscovite-tourmaline-garnet orthogneiss	75 (1)	14.6 (0.6)	4.3 (0.3)	27.9 (0.9)
Tis Pluton, S-type						
3315	Lubenec outcrop	Biotite granodiorite	65.7 (0.6)	14.7 (0.2)	1.48 (0.06)	19.1 (0.4)
4658	Lubenec outcrop	Biotite granodiorite	72.9 (0.8)	13.3 (0.2)	1.5 (0.1)	20 (1)
3230	Outcrop Bába near Žihle	Biotite granite	73.9 (0.8)	13.3 (0.2)	1.3 (0.2)	18 (1)
3231	Quarry Tis	Biotite granite	73.7 (0.4)	13.1 (0.1)	1.44 (0.08)	18.3 (0.3)
4653	Quarry Stebno	Biotite granite	67.5 (0.7)	14.87 (0.3)	1.9 (0.2)	20.8 (0.6)
Central Bohemian Pluton, I-type						
4848	Quarry Něčín	Biotite-hornblende granodiorite	74 (1)	13.8 (0.3)	1.50 (0.09)	14.3 (0.6)
4849	Quarry Krhanice	Biotite trondhjemite	63.6 (0.7)	18.8 (0.3)	1.6 (0.1)	16.8 (0.3)
4845	Quarry Kozárovice	Biotite-hornblende granodiorite	65.5 (0.8)	15.2 (0.2)	1.7 (0.1)	19.8 (0.3)
4846	Quarry Hudčice	Biotite-hornblende granodiorite	63.0 (0.9)	15.5 (0.3)	1.8 (0.1)	21.6 (0.9)
4847	Quarry Vápenice	Biotite granodiorite	66 (1)	14.3 (0.4)	2.1 (0.2)	21.1 (0.5)
4850	Quarry Žernovka	Biotite granite	69 (1)	15.8 (0.2)	2.1 (0.2)	24.7 (0.4)
South Bohemian Pluton, S-type						
4084	Melechov massif, Šafranice hill, outcrop	Biotite (± muscovite) granite of Lipnice type	71.3 (0.8)	15.2 (0.3)	1.8 (0.1)	24.8 (0.4)
4231	Melechov massif, quarry Lipnice	Biotite (± muscovite) granite of Lipnice type	70.0 (0.5)	14.8 (0.2)	1.7 (0.2)	24.5 (0.6)
2793	Melechov massif, quarry Březinka	Two-mica granite of Kouty type	72.0 (0.7)	14.7 (0.1)	1.5 (0.2)	22 (1)
4265	Melechov massif, Svatojánské hutě, outcrop	Two-mica granite of Kouty type	71 (1)	15.3 (0.3)	1.0 (0.1)	21.2 (0.7)
4089	Melechov massif, outcrops near Rohole	Two-mica granite of Eisgarn type	72.0 (0.4)	15.6 (0.2)	2.2 (0.2)	20.4 (0.4)
4093	Melechov massif, outcrops near Rohole	Two-mica granite of Eisgarn type	71.5 (0.6)	15.9 (0.2)	2.2 (0.1)	21.7 (0.7)
2772	Central massif, Kozí hora quarry	Fine-grained biotite granite with molybdenite	72.7 (0.6)	14.9 (0.2)	1.3 (0.1)	22.4 (0.4)
2761	Central massif, Lodhéřov, outcrop	Two-mica granite of Lásenice type	73.9 (0.8)	14.3 (0.3)	1.8 (0.1)	16.6 (0.6)
2771	Central massif, Kardašova Řečice quarry	Two-mica granite of Lásenice type	75.1 (0.6)	13.8 (0.3)	1.6 (0.1)	18.7 (0.5)
2782	Central massif, Mysletice quarry	Two-mica granite of Mrákotín type	72 (1)	14.8 (0.2)	1.6 (0.1)	22.1 (0.5)
3024	Central massif, quarry Mrákotín	Two-mica granite of Mrákotín type	73.3 (0.4)	14.1 (0.1)	1.3 (0.3)	24.1 (0.9)
2774	Central massif, Stálkov outcrop	Porfyritic two-mica granite Číměř type	74.3 (0.7)	13.7 (0.2)	1.7 (0.4)	23.9 (0.8)
2944	Central massif, Rožnov outcrop	Porfyritic two-mica granite Číměř type	70.7 (0.7)	14.9 (0.2)	1.5 (0.1)	26.3 (0.4)
2962	Central massif, Langeg quarry	Porfyritic two-mica granite Číměř type	73.9 (0.8)	14.3 (0.3)	1.6 (0.1)	25.9 (0.5)
3009	Central massif, Číměř quarry	Porfyritic two-mica granite Číměř type	73 (1)	14.3 (0.1)	1.8 (0.2)	23.7 (0.6)
2777	Central massif, Zvůle outcrop	Two-mica granite of Zvůle type	72.9 (0.8)	14.4 (0.2)	1.7 (0.1)	22.4 (0.7)
2940	Central massif, Valtinov outcrop	Two-mica granite of Eisgarn type	72 (1)	14.3 (0.4)	1.8 (0.1)	22.8 (0.8)
2949	Central massif, Griesbach outcrop	Two-mica granite of Eisgarn type	71.3 (0.6)	15.0 (0.2)	1.8 (0.2)	25.3 (0.6)
2954	Central massif, Grasselstein outcrop	Two-mica granite of Eisgarn type	74 (1)	14.1 (0.2)	2.3 (0.2)	27.3 (0.5)
2964	Central massif, Dreichsbach valley, outcrop	Two-mica granite of Eisgarn type	71.3 (0.7)	14.6 (0.2)	2.8 (0.2)	26.8 (0.6)
2511	Central massif, Homolka hill, outcrop	Albite-Muscovite-Topaz granite	73.6 (0.6)	14.8 (0.2)	4.2 (0.2)	29.1 (0.5)
2512	Central massif, Homolka hill, outcrop	Albite-Muscovite-Topaz granite	72.8 (0.4)	15.1 (0.2)	5.4 (0.1)	26.4 (0.4)
2513	Central massif, Homolka hill, outcrop	Albite-Muscovite-Topaz granite	74.3 (0.8)	14.5 (0.6)	6.2 (0.2)	31.0 (0.6)
2476.	Central massif, debris Šejby	Pegmatoidal muscovite-garnet granite	73 (1)	14.3 (0.3)	5.5 (0.2)	33.1 (0.9)
2613	Central massif, debris Šejby	Pegmatoidal muscovite-garnet granite	73.4 (0.5)	15.5 (0.5)	4.5 (0.2)	35.1 (1)
4139	Plechý massif, outcrop Teufelschussel	Th-rich biotite (± muscovite) granite	71 (1)	14.2 (0.3)	1.7 (0.1)	29.4 (0.6)
4362	Plechý massif, outcrop Hebergrasberg hill	Th-rich biotite (± muscovite) granite	71.8 (0.2)	14.5 (0.2)	1.42 (0.03)	27.6 (0.1)
4368	Plechý massif, outcrop Trojmezná hill	Two-mica granite of Eisgarn type	73.6 (0.7)	14.4 (0.2)	1.6 (0.1)	21.3 (0.4)
3612	Plechý massif, debris near Pěkná	Two-mica granite of Eisgarn type	73.2 (0.2)	14.9 (0.1)	1.9 (0.1)	24.3 (0.6)
4363	Plechý massif, outcrop Dreisessel hill	Two-mica granite of Eisgarn type	73.2 (0.6)	14.0 (0.2)	1.7 (0.2)	33.0 (0.8)
4365	Plechý massif, outcrop Kamenná hill	Two-mica granite of Eisgarn type	72.4 (0.4)	14.3 (0.5)	1.6 (0.1)	23.7 (0.2)
Nejdek Pluton, S-type granites						
2924	Quarry Horní Rozmyšl	Biotite granite	72.4 (0.6)	13.9 (0.2)	2.2 (0.2)	20.1 (0.4)
2925	Quarry Mezihorská	Biotite granite	71.1 (0.6)	14.4 (0.2)	2.0 (0.3)	21.7 (0.8)
4742	Outcrop Dračí skála	Biotite granite	71.5 (0.4)	14.2 (0.4)	1.5 (0.2)	22.5 (0.7)
4743	Outcrop Tisovský vrch hill	Biotite granite	72 (1)	14.7 (0.7)	1.3 (0.1)	22.4 (0.5)
4744	Outcrop Bílá skála	Biotite granite	74.8 (0.9)	13.3 (0.6)	1.2 (0.1)	27.0 (0.6)
4745	Quarry in the Černá valley	Li-enriched biotite granite with topaz	72.5 (0.8)	15.0 (0.3)	2.8 (0.3)	35.0 (0.8)
Podlesí stock, S-type granites						
3475	Podlesí, borehole PTP-3, depth of 199 m	Albite-Biotite granite	73.6 (0.9)	14.3 (0.3)	3.6 (0.5)	37.2 (0.6)
3490	Podlesí, borehole PTP-3, depth of 232 m	Albite-Biotite granite	73.8 (0.9)	14.6 (0.2)	5.0 (0.2)	37.5 (0.5)
3385	Podlesí, outcrop	Albite-Protolithionite-Topaz granite	73.8 (0.2)	14.6 (0.1)	3.4 (0.1)	32.5 (0.5)
3458	Podlesí, borehole PTP-3, depth of 82 m	Albite-Protolithionite-Topaz granite	73.2 (0.8)	14.8 (0.2)	3.6 (0.4)	36 (1)
3464	Podlesí, borehole PTP-3, depth of 106 m	Albite-Protolithionite-Topaz granite	73.7 (0.8)	14.4 (0.2)	3.6 (0.4)	34 (1)

Table 2: *Continued from the previous page.*

No.	Locality	Description	SiO_2	Al_2O_3	Ge	Ga
Podlesí stock, S-type granites			**wt. % (SD)**	**wt. % (SD)**	**ppm (SD)**	**ppm (SD)**
3511	Podlesí, borehole PTP-3, depth of 348 m	Albite-Protolithionite-Topaz granite	72.6 (0.7)	14.8 (0.2)	4.1 (0.2)	34.4 (0.5)
3413	Podlesí, quarry	Albite-Zinnwaldite-Topaz granite	73 (2)	16 (1)	3.9 (0.2)	52.6 (0.8)
3414	Podlesí, quarry	Albite-Zinnwaldite-Topaz granite	70.7 (0.9)	15.9 (0.8)	4.4 (0.3)	54.5 (0.5)
3416	Podlesí, quarry	Albite-Zinnwaldite-Topaz granite	70 (1)	15.8 (0.5)	3.9 (0.3)	69 (1)
3417	Podlesí, quarry	Albite-Zinnwaldite-Topaz granite	66.5 (0.7)	17.8 (0.4)	4.4 (0.4)	77 (1)
3366	Podlesí, outcrop	Biotite-Topaz greisen	77.6 (0.6)	14.9 (0.2)	8.8 (0.4)	10.9 (0.5)
3387	Podlesí, outcrop	Zinwaldite-Topaz greisen	82 (2)	13.2 (0.9)	7.6 (0.6)	7.8 (0.6)
Hora Svaté Kateřiny, A-type granites						
4471	Hora Svaté Kateřiny stock, debris	Albite-Biotite granite	76.6 (0.8)	12.2 (0.2)	2.5 (0.2)	31.7 (0.9)
4604	Hora Svaté Kateřiny stock, debris	Albite-Biotite granite	77.1 (0.6)	12.6 (0.2)	3.1 (0.3)	40.1 (0.1)
3097	Hora Svaté Kateřiny stock, debris	Albite-Zinnwaldite granite	74.2 (0.5)	13.2 (0.3)	3.7 (0.1)	38.3 (0.9)
4554	Hora Svaté Kateřiny stock, debris	Albite-Zinnwaldite granite	75.5 (0.7)	12.6 (0.3)	3.4 (0.3)	37.7 (0.7)
Teplice caldera, A-type rocks						
3194	Mikulov, borehole Mi-4, depth of 50 m	Rhyolite ignimbrite	76 (1)	12.3 (0.6)	1.6 (0.3)	21 (1)
3198	Mikulov, borehole Mi-4, depth of 178 m	Rhyolite ignimbrite	74.7 (0.4)	12.3 (0.2)	1.4 (0.3)	20 (1)
3201	Mikulov, borehole Mi-4, depth of 285 m	Rhyolite ignimbrite	76.4 (0.5)	12.3 (0.2)	1.13 (0.06)	18.1 (0.2)
3207	Mikulov, borehole Mi-4, depth of 483 m	Rhyolite ignimbrite	77.1 (0.8)	11.6 (0.2)	2.3 (0.2)	24.4 (0.8)
3208	Mikulov, borehole Mi-4, depth of 512 m	Rhyolite ignimbrite	76.4 (0.8)	11.8 (0.4)	1.4 (0.1)	20.3 (0.6)
3210	Mikulov, borehole Mi-4, depth of 579 m	Rhyolite ignimbrite	75.8 (0.7)	12.2 (0.1)	1.9 (0.1)	21.2 (0.4)
3211	Mikulov, borehole Mi-4, depth of 608 m	Rhyolite ignimbrite	61 (1)	24.4 (0.5)	2.3 (0.2)	32 (1)
3532	Loučná hill outcrop	Granite porphyry	68.9 (0.5)	14.7 (0.1)	1.9 (0.1)	23.9 (0.2)
3376	Frauenstein outcrop	Granite porphyry	68.1 (0.8)	14.7 (0.3)	1.7 (0.1)	23.7 (0.6)
4686	Cínovec, borehole CS-1, depth of 336 m	Albite-Zinnwaldite granite	76 (2)	13.6 (0.7)	2.9 (0.3)	47 (1)
4687	Cínovec, borehole CS-1, depth of 413 m	Albite-Zinnwaldite granite	76 (2)	12.5 (0.4)	3.0 (0.4)	40 (1)
4691	Cínovec, borehole CS-1, depth of 749 m	Biotite granite	76 (1)	12.8 (0.1)	2.8 (0.2)	35 (1)
4692	Cínovec, borehole CS-1, depth of 988 m	Biotite granite	75 (2)	12.5 (0.2)	1.5 (0.2)	28.9 (0.9)
4693	Cínovec, borehole CS-1, depth of 1579 m	Biotite granite	76 (2)	12.6 (0.4)	1.7 (0.1)	32.4 (0.7)

gneisses during the Variscan orogeny (intrusive age ca. 508 Ma; Vrána & Kröner 1995). This complex comprises more than 20 bodies of biotite, two-mica and muscovite-garnet-tourmaline orthogneisses, the latter of which are enriched in Na, P, B, and Sn (Breiter et al. 2005a).

The Tis Pluton (504 Ma; Venera et al. 2000) is a typical representative of the Cambro-Ordovician peraluminous geochemically primitive granites in the Teplá-Barrandian area in Western Bohemia. The unmetamorphosed and only locally slightly deformed Tis pluton is composed of biotite granodiorite and biotite granite (Breiter 2004).

The Central Bohemian Pluton (CBP) situated in the south-central part of the Czech Republic is a typical composite pluton of I-type (350–336 Ma; Holub et al. 1997a,b; Janoušek & Skála 2011). It comprises intrusive suites of different geochemical types: (i) calc-alkaline mostly metaluminous amphibole-biotite tonalites and quartz diorites to biotite trondhjemites and granodiorites with associated basic rocks (*Sázava suite*); (ii) high-K calc-alkaline biotite ± amphibole granodiorites and granites (*Blatná suite*); (iii) highly K, Mg-enriched amphibole-biotite melasyenites and melagranites (durbachites) and associated K, Mg-rich biotite granites (*Čertovo břemeno suite*); and (iv) peraluminous biotite (± muscovite) granites (*Říčany suite*). The Sázava suite is supposed to represent the melting of reworked material originating from a depleted mantle wedge and subducted oceanic sediments, while rocks from the Blatná suite were generated by the remelting of heterogeneous Neoproterozoic and Cambrian crust (Janoušek & Skála 2011). The high-K, Mg melagranitoids (durbachites) are believed to be the product of the melting of the metasomatized upper mantle (Holub et al. 1997b).

The South Bohemian Pluton is a complex of Variscan peraluminous granites in southern Bohemia and northern Austria (330–315 Ma). The pluton is composed of several composite plutons; the largest are the Melechov Massif on the north (Breiter & Sulovský 2005), the Central Massif on the SE (Breiter & Koller 1999) and the Plechý Massif on the SW (Breiter et al. 2007a). Petrographically, the pluton comprises slightly deformed biotite > muscovite granites of Lipnice type, slightly deformed two-mica granites of Lásenice type, undeformed two-mica granites (Mrákotín, Čiměř and Aalfang types), younger fractionated two-mica granites (Eisgarn type s.s. according to Waldmann 1950) and topaz-muscovite granites enriched in Na, P, F, Rb, Sn and Nb. All these rocks represent the product of voluminous melting of crustal rocks (Breiter & Scharbert 1995; Finger et al. 1997; Gerdes et al. 1998). The Weinsberg and Mauthausen massifs (Finger et al. 1997) located further to the south in Austria are not included in this study.

The Nejdek Pluton is the most typical example of a strongly peraluminous rare metal-bearing pluton in the western Krušné Hory/Erzgebirge area. This pluton is composed of two suites traditionally described as "intrusive complexes". The older intrusive complex is composed of several textural types of biotite granites, while the younger intrusive complex comprises biotite granites followed by intrusions of F, P, Li, Rb, Sn, and U-enriched Li-mica-topaz granites (ca. 330–312 Ma; Breiter et al. 1999; Förster et al. 1999). This evolution terminated in the extremely fractionated P-, F-, Na-, Li-, Sn-, Nb-,

Ta-, and W-enriched Podlesí stock with examples of layered rocks, unidirectional solidification textures and greisenization (Breiter et al. 2005b).

The Hora Svaté Kateřiny intrusion forms a small stock of strongly fractionated subvolcanic A-type granites in the central part of the Krušné hory/Erzgebirge (308 Ma; Breiter 2008).

The late-Variscan A-type volcano-plutonic complex of the eastern Erzgebirge (Altenberg-Teplice caldera) comprises comagmatic slightly peraluminous "Teplice rhyolite" (309 Ma; Hoffmann et al. 2013) and slightly younger rare metal granites of the Cínovec Pluton (Breiter 2012).

Contents of Si, Al, K, Ga and Ge, as well as some trace elements, were analysed in typical whole-rock samples representing the magmatic evolution of all of the aforementioned plutons (Table 2).

Analytical methods

Contents of Al, Si, Ga and Ge were determined using ICP-MS in the laboratory of the Department of Chemistry, Masaryk University Brno, Czech Republic. Whole-rock granitoid samples and the certified reference material (CRM GBW07406, National Reasearch Center for CRMs, China) were decomposed using fusion with $LiBO_2$ (Spectromelt A20, Merck), (0.2 g of a sample with 1.0 g of $LiBO_2$). The resulting borosilicate glass bead was dissolved under stirring in 20 ml of 0.7 mol/l HNO_3, the solution was transferred into a volumetric flask and after addition of internal reference element (Se) filled up 250 ml with deionized water. Blank solutions were prepared in the same way as the samples. The set of 6 calibration solutions containing Ga and Ge in the range from 0 to 200 µg/l were used for their determination in samples. For suppressing of matrix effect caused by HNO_3 all the calibration solutions were prepared using 0.06 mol/l HNO_3 and selenium was used as an internal standard. The ICP spectrometer (Agilent, 7500CE, Sta Clara, CA, USA) is equipped with collision-reaction cell for suppressing possible isobaric interferences. The generator power input was 1500 W, outer plasma gas flow rate (Ar) 15.0 $l \cdot min^{-1}$, intermediate plasma gas flow rate (Ar) 0.25 $l \cdot min^{-1}$, carrier gas (Ar) flow-rate 0.85 $l \cdot min^{-1}$, sample flow rate 200 $\mu l \cdot min^{-1}$, nebulizer temperature 2 °C and He flow-rate in collision cell was 3 $ml \cdot min^{-1}$. The following isotopes were recorded for Al, Si, Ga and Ge determination: ^{27}Al, ^{28}Si, ^{69}Ga, ^{71}Ga, ^{72}Ge and ^{73}Ge. Due to strong isobaric interferences $^{29}Si^{40}Ar$ and $^{16}O^{56}Fe$, which was suppressed insufficiently by collision reaction cell, the isotopes ^{71}Ga and ^{73}Ge were only used for determination. For quality control the CRM GBW7406 was analysed in each set of dissolved samples.

The content of potassium was analysed in the laboratory of the Czech Geological Survey, Prague using the atomic absorption method. Replicate analyses of international reference material (JG-3 granodiorite; Geological Survey of Japan) yield an average error (1 σ) of ±1 % with respect to recommended values (Govindaraju 1994). The trace elements (Rb, Y, Ho) were determined by ICP mass spectrometry following a lithium metaborate/tetraborate fusion and nitric acid digestion of a 0.2 g sample in the laboratory of ACME, Vancouver, Canada. (Details in http://acmelab.com/.)

The accuracy of determination of Ga and Ge was checked by analysis of CRM GBW7406. The results of Ga and Ge determination and their limits of detection (LOD) are given in Table 3. The average content is calculated from 6 analyses of the CRM. Accuracy was statistically tested and no significant differences between certified and determined values were found. LOD was calculated according to IUPAC 3σ definition.

$$LOD = \frac{3\sigma_{bl}}{S};$$

where $3\sigma_{bl}$ is standard deviation of blank calculated from 5 replicates, S is slope of calibration line of given isotope.

Table 3: Results of determination of Ga and Ge in certified reference material GBW7406.

	Ga	Ge
Measured content [mg/kg]	32 ± 2	3.4 ± 0.3
Certified value [mg/kg]	30 ± 3	3.2 ± 0.3

Results

The contents of Al, Si, Ga and Ge, including their standard deviations, in the analysed granites, rhyolites and orthogneisses are summarized in Table 2 and illustrated in Fig. 2. It follows from Table 2 that the contents of Ge and Ga are well above their LODs. The complete data set used for figure constructions is accessible as an electronic attachment.

The Al-contents in A-type rocks is distinctly lower (6.6–7.2 wt. % Al, 12.5–13.6 wt. % Al_2O_3) than in S- and I-type rocks (7.0–8.4 wt. % Al, 13.3–15.9 wt. % Al_2O_3). The content of 6.8 wt. % Al (12.85 wt. % Al_2O_3) can serve as useful value for discrimination of A-type granitoids.

The content of Si in A-type granites (mostly 34.7–36.0 wt. % Si, 74.2–77.1 wt. % SiO_2) is generally higher than those in S-type granites (mostly 33.0–34.5 wt. % Si, 70.7–73.7 wt. % SiO_2) and I-type rocks (29.4–34.6 wt. % Si, 63–74 wt. % SiO_2). Only several samples have Si-contents outside the aforementioned intervals: quartz-rich greisen of S-type granites (up to 38.3 wt. % Si, 81.8 wt. % SiO_2), some S-type granodiorites (down to 30.6 wt. % Si, 65.7 wt. % SiO_2) and A-type granite porphyry (down to 31.8 wt. % Si, 68.1 wt. % SiO_2). The content of 35 wt. % Si (ca. 75 wt. % SiO_2) can discriminate the majority of the A-type rocks.

The Ga contents in the studied samples range from 7.8 to 77.4 ppm. The values for the less- and moderately fractionated rock types range from 14 to ca. 35 ppm. Higher values were found in strongly fractionated rare-metal A-type granites (up to 47 ppm) and strongly peraluminous S-type granites (up to 77 ppm). The lowest contents were found in hydrothermal greisens of peraluminous granites (less than 10 ppm). The Al/1000Ga values varied between 1.2 and 5.9 in granites and rhyolites, between 2.8 and 4.4 in orthogneisses, and between 7.2 and 9 in greisens.

The Ge contents vary from 1.0 to 8.8 ppm. Most of the less and moderately fractionated granitoids exhibited ranges

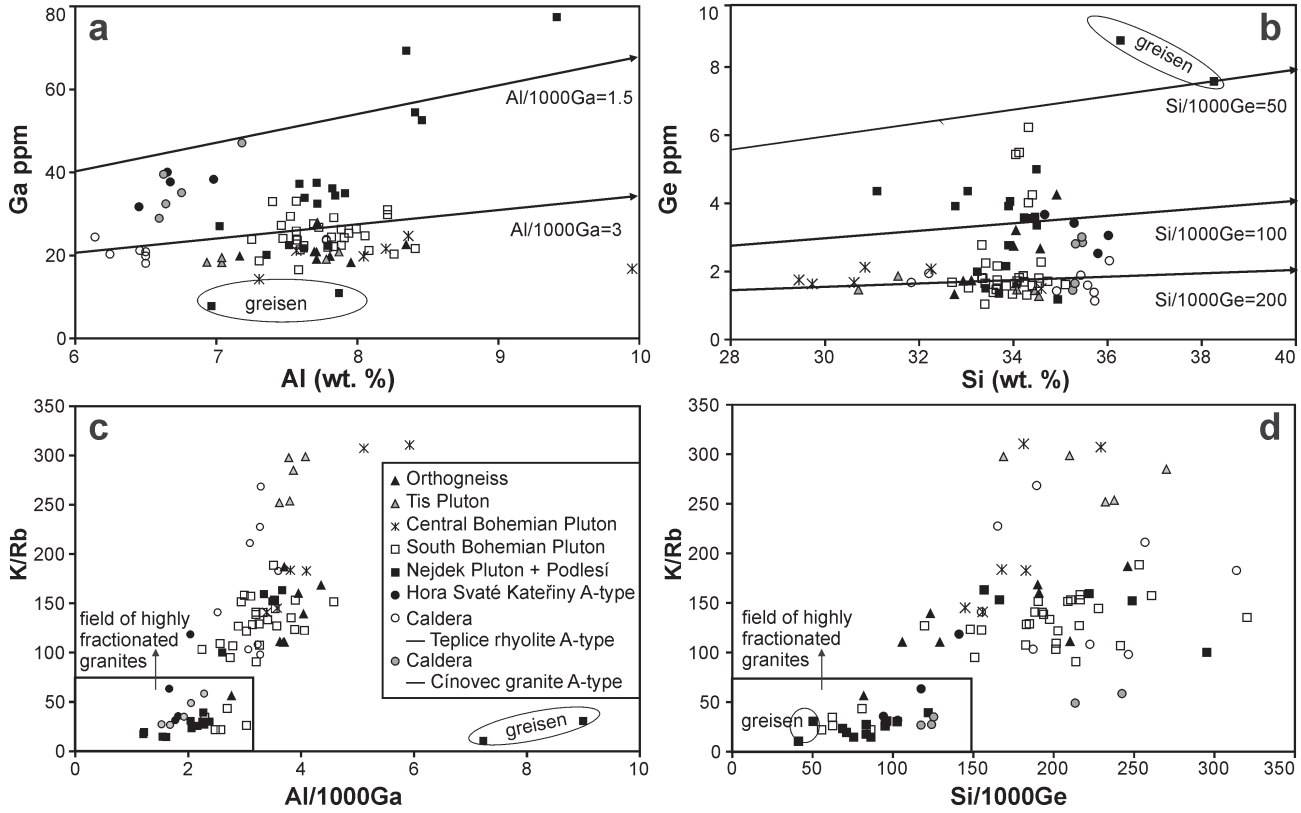

Fig. 2. a — Graph of Al vs. Ga. The highest Ga contents were detected in extremely fractionated facies of S-type granites in the western part of the Krušné Hory Mountains. The lowest contents of Ga were found in greisens. The contents of Al are slightly lower in A-type granitoids. The Al/Ga values are depicted in the right part of the graph. **b** — Graph of Si vs. Ge. The Ge content increases only slightly during the differentiation of plutons from 1–2 ppm to 4–5 ppm. The highest Ge contents were found in quartz-topaz greisens (7–9 ppm). The Si/Ge values are depicted in the right of the graph. **c** — Graph Al/1000Ga vs. K/Rb illustrates changes in the Al/Ga-ratio during evolution of individual plutons. **d** — Graph Si/1000Ge vs. K/Rb illustrates changes in the Si/Ge-ratio during evolution of individual plutons.

of 1.5 to 2.5 ppm, and the highly fractionated ones had ranges of 2.5 to 5 ppm. The highest values, 7.6 and 8.8 ppm, were found in metasomatic greisens. The Si/1000Ge ratio varies from 100 to 320 in less fractionated granites and rhyolites and from 69 to 125 in highly fractionated granites. The Si/1000Ge values in orthogneisses are similar to those of granites, ranging from 81.8 to 246. The lowest Si/1000Ge values (41–50) were found in greisens of peraluminous granites.

Discussion

In more places through the text we use the term "fractionated granites". This term refers to rocks to varying degrees enriched with some LILE (large-ion lithophile elements like K, Rb, Cs), HFSE (high field strength elements like U, Nb, Ta, Sn, W) and fluxing agents (F, P, H_2O) which generally underwent long fractional crystallization from the primary melt. These rocks are also called "specialized granites" or "rare-metal granites". From the mineralogical point of view, they are usually composed of albite, K-feldspar, quartz, Li-bearing mica and topaz (or fluorite). For this group of rocks there is no universally applicable index of fractionation. Increase of silica, widely used for this purposes in Harker's diagrams, is not applicable here. In the most evolved peraluminous rocks, due to enrichment in alkalis, fluorine and phosphorus, silica decreases (Förster et al. 1999; Breiter et al. 2005b). Förster et al. (1999) proposed to use for this purpose the value $1/TiO_2$. According to our opinion, the traditional K/Rb-value is well applicable marker of fractionation for all geochemical types of rock (I-, S- and A-types) and it is applied in this paper. We use the term "fractionated granites" for rocks with K/Rb <75.

Changes in Al/Ga and Si/Ge values during pluton evolution

The most widely used chemical indicator of evolution of magmatic rocks is the K/Rb value (Clarke 1992). Rubidium has a larger ionic radius than the potassium, making it less compatible with the crystal lattice of common K-bearing silicates. As a consequence, K preferentially concentrates in crystallizing minerals during melt crystallization, while Rb remains in the residual melt. This results in a systematic decrease in K/Rb value during fractional evolution of the parental melt.

Our study includes plutons composed of (i) suits with different protoliths (Central Bohemian Pluton), (ii) group of repeated intrusions from the same source (Nejdek Pluton,

Teplice caldera), and (iii) plutons combining both these principles (South Bohemian Pluton, Rozvadov Pluton). In all these cases, decrease of the K/Rb value clearly illustrates the general geochemical evolution of the pluton: K/Rb decreases from 300 in the early down to 20 in the final products of magmatic evolution.

The differences in ionic radii and ionization potentials between Si and Ge and between Al and Ga indicate that a relative Ge and Ga enrichment of residual melts should be expected (Goldschmidt 1937; Wedepohl 1972). As result, the Si/Ge and Al/Ga values will decrease during fractionation. Argollo & Schilling (1978) demonstrated that during the crystallization of Hawaiian basalts, an increase of Ga and Ge contents was simultaneously accompanied by an increase of Al and Si contents; as a result, no systematic changes in Si/Ge or Al/Ga values were observed in these basalts. In contrast, all studied granitic plutons from the Bohemian Massif show distinct decrease in both ratios during fractionation, as theoretically expected.

During magmatic evolution of individual plutons, the Al/Ga values generally decreased due to an increase in Ga, but increased during post-magmatic high-temperature hydrothermal greisenization due to a strong decrease in Ga (Fig. 2c). For example, the Al/1000Ga-value decrease in the I-type Central Bohemian Pluton from 5.1–5.9 in tonalites of the Sázava-suite through 3.8–4.1 in granodiorites of the Blatná suite to 3.4 in the Říčany granite. In the S-type granites from the Nejdek Pluton, this value decreased from 3.5–3.7 in the older biotite granites down to 1.2 in the younger albite-zinnwaldite granites. Similarly in the A-type caldera system, the Al/1000Ga value decreased from ca. 3.5 in rhyolites to <2 in zinnwaldite granites. On the other side, in the S-type South Bohemian Pluton this value scattered without any distinct trend.

Whalen et al. (1987) considered the Al/Ga ratio to be critical for distinguishing A- and S-type granitoids. According to our results, this criterion cannot be applied generally. The highest Ga contents were detected in strongly peraluminous S-type granites: up to 67 ppm Ga (Al/1000Ga = 2.6) in a topaz-lepidolite granite at Beauvoir, France (Raimbault et al. 1995) and 77 ppm Ga (Al/1000Ga = 1.2) in albite-zinnwaldite granite at Podlesí, Czech Republic (this paper). This is more than in the A-type granites from the Erzgebirge (32–47 ppm Ga, Al/1000Ga = 1.5–2.3; this paper) or in the highly fractionated A-type Madeira Complex in Brazil (max. 59 ppm Ga, Al/1000Ga = 2.2; Lenharo et al. 2003). Differences in the ionic potentials of Al and Ga are particularly manifested in water- and F-rich residual melts where a distinct relative enrichment with Ga occurs, regardless of the geochemical type of parental magma. In contrast, the lowest contents of Ga (7.8–10.9 ppm) and thus the highest Al/1000Ga value (ca. 8) were found in greisens of peraluminous granites where Ga was released during the hydrothermal decomposition of feldspars and partitioned into a fluid phase. While Al was immediately incorporated into newly formed topaz, Ga was washed out from the rock.

The Si/1000Ge ratio decreases during magmatic evolution of some plutons, such as in the S-type Nejdek Pluton from the western Erzgebirge (from ca. 295 in biotite granites to ca. 70 in albite-zinnwaldite granite), in the A-type caldera granites from the eastern Erzgebirge (from ca. 240 in biotite granite to ca. 120 in zinnwaldite granite) and in the I-type Central Bohemian Pluton (from 229 in the Sázava tonalite to 156 in the Říčany granite). In the S-type South Bohemian Pluton the Si/1000Ge value scattered between 320 and 56 without correlation with the K/Rb value. But when we examine the samples from the South Bohemian Pluton in more detail (Fig. 3), we find out that the dispersion of data has a geological background:

Samples from the Central Massif form one array, with positive correlation between Si/Ge- and K/Rb-values. We conclude that all these rock samples are products of fractionation from one parental melt. The only sample positioned outside this array is slightly altered and thus impoverished in Rb.

The samples from the Melechov Massif form three groups corresponding to different textural facies within the massif: the fine-grained two mica granite of Kouty type (Si/1000Ge = 320), fine-grained biotite > muscovite granite

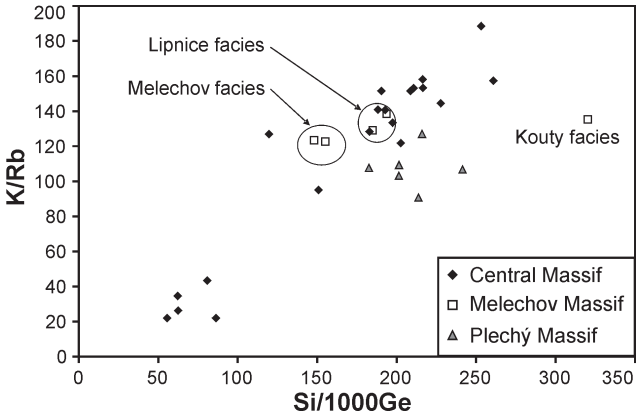

Fig. 3. Graph Si/1000Ge vs. K/Rb shows differences in geochemical evolution of individual magmatic centers within the South Bohemian Pluton.

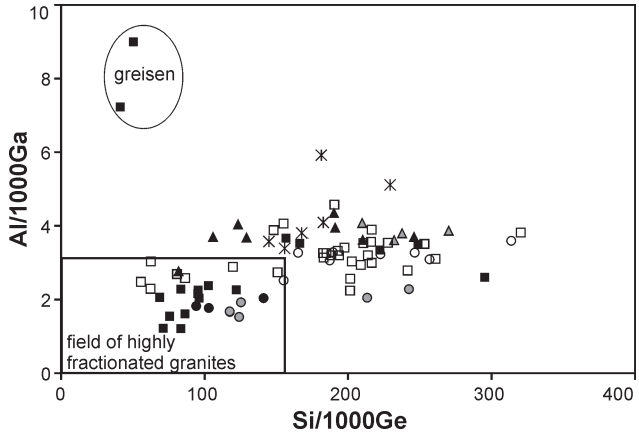

Fig. 4. Graph of Al/Ga versus Si/Ge ratios for comparison of evolution of both values. The Si/Ge ratio more accurately illustrates the general process of differentiation. Empirical field of highly fractionated granites with limits Si/1000Ge < 150 and Al/1000Ga < 3 is depicted. Greisens lie outside the magmatic trend. For symbol descriptions, see Fig. 2.

of Lipnice type (Si/1000Ge = 185–194) and coarse-grained two-mica granite of Melechov type (148–155). In this case, different enrichment in Ge, at the same K/Rb-value, may result from differences in protolith involved in melting of individual intrusions.

In the case of the Plechý Massif, the scatter in both Si/Ge- and K/Rb-values does not correspond to textural facies distinguished within the massif (Breiter et al. 2007a) and should be interpreted as a result of the internal inhomogeneity of this intrusive body.

When comparing the Si/Ge and Al/Ga ratios (Fig. 4), the Si/Ge ratio more accurately illustrates the general process of differentiation, which meant evolution from the primitive to the more evolved melts. The same trend also follows during high-temperature greisenization. The Al/Ga value can better discriminate the latest highly fractionated rocks. However, this value varies considerably in the crystallization products of the late F-rich melts at Podlesí (enrichment in albite-rich layered rocks) and products of hydrothermal alteration (decrease in greisens).

The Ge and Ga contents of Moldanubicum orthogneisses correspond to their overall contents in granites of similar composition, which indicates that neither element was considerably redistributed during regional amphibolite-facies metamorphism.

Changes in water-rich melts and during hydrothermal processes

The Y/Ho value changes little during fractional crystallization of silicate melts. However, this ratio appears to be sensitive to processes occurring in residual water-rich melts associated with the admixture of fluids (Bau 1996; Irber 1999).

A graph showing the Al/Ga vs. Y/Ho ratios (Fig. 5) illustrates the dissimilarity of various processes occurring during the late stages of development of fractionated granites. The majority of analysed S-type granite samples fall in a narrow interval for both ratios that correspond to fractional crystallization of a common granite melt: the Al/1000Ga ratio ranges from 4.5 to 1.5, and the Y/Ho ratio ranges from 30 to 40.

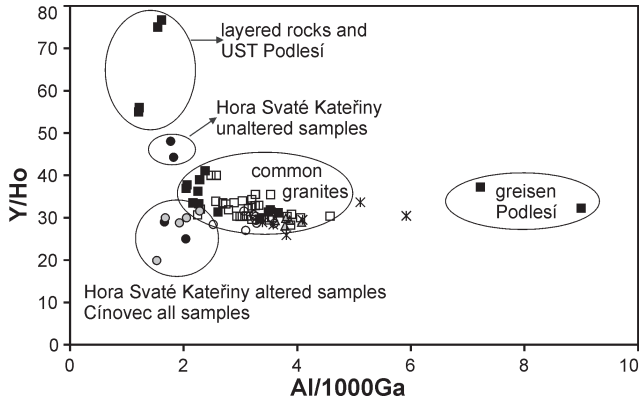

Fig. 5. Graph of Al/Ga versus Y/Ho ratios illustrates dissimilarity of various processes occurring in the late evolution of granites. See the text for explanation. For symbol descriptions, see Fig. 2.

Two samples with high Al/Ga values represent quartz-topaz greisens of a metasomatic nature, formed when Ga was removed with the fluid phase during the alteration and decomposition of primary feldspars and micas, while Al remained fixed in authigenic micas and topaz. Four samples with low Al/Ga ratios and the highest Y/Ho values represent the terminal stage of fractional crystallization of an S-type melt rich in Na, F and water. In this case, the Ga content increased (Al/1000Ga < 1.5), and the melt became completely depleted of Ho, which entered zircon and, to a lesser extent, xenotime, while some Y remained in the melt (Y/Ho > 50). A-type granites in the Bohemian Massif are represented only with strongly fractionated facies with low Al/Ga values. However, even in this particular case, the Y/Ho values enable us to distinguish rocks that underwent only fractional crystallization from the melt (Y/Ho = 40–50), from rocks with miaroles, which argues for the admixture of a fluid phase from the melt (Y/Ho = 25–30). During this stage, xenotime, which was the primary host of HREE, was destroyed, and secondary REE minerals (fluorides, oxyfluorides and fluorocarbonates) were immediately formed. During this process, Y is more mobile than Ho (Breiter et al. 2009), which results in a decrease in the Y/Ho value in the rock (Y/Ho = 25–32).

Conclusions

The main results of this study of the distribution and behaviour of Ga and Ge in granites can be summarized as follows:

- Gallium contents vary from 16 to 77 ppm in the studied granitoids, and from 8 to 11 ppm in greisens.
- Germanium contents range from 1 to 5 ppm in granitoids and from 8 to 9 ppm in greisens.
- During fractionation, magma becomes relatively enriched with Ga and Ge, while the Si/Ge and Al/Ga values decrease.
- Gallium contents and Al/Ga values can be used to distinguish A- and S-type granitoids only in a very limited way.
- The maximum Ga enrichment occurs at the end of fractionation of water- and F-rich melts, where the differences between the ionic radii and complexation potentials of Ga and Al become more distinct. The maximum contents of Ge were detected in metasomatic greisens.
- During hydrothermal greisenization, Ga becomes dispersed while Ge is conserved in newly crystallizing quartz and topaz.
- The metamorphism of amphibolite facies has no visible effect on the distribution of Ge or Ga.
- The Al/Ga vs. Y/Ho diagram seams to be useful tool for discrimination of different kinds of highly evolved granitic melt and products of their hydrothermal alteration.

Acknowledgments: This investigation was supported by the Czech Science Foundation, Project No. P210/10/1309, RVO 67985831 and Project CEITEC (CZ.1.05/1.1.00/02.0068) from the European Regional Development Fund. Comprehensive reviews by Igor Petrík and Jean-Clair Duchesne and remarks by Igor Broska are acknowledged.

Referenecs

Anders E. & Grevesse N. 1989: Abundances of the elements: Meteoritic and solar. *Geochim. Cosmochim. Acta* 53, 197–214.

Argollo R.D. & Schilling J.G. 1978: Ge-Si and Ga-Al fractionation in Hawaian volcanic rocks. *Geochim. Cosmochim. Acta* 42, 623–630.

Bau M. 1996: Controls on the fractionation of isovalent trace elements in magmatic and aqueous systems: Evidence from Y/Ho, Zr/Hf, and lanthanide tetrad effect. *Contr. Mineral. Petrology* 123, 323–333.

Bernstein L.R. 1985: Germanium geochemistry and mineralogy. *Geochim. Cosmochim. Acta* 49, 2409–2422.

Best M.G. 2003: Igneous and metamorphic petrology. *Blackwell Publishing*, 1–729.

Breiter K. 2004: Granitoids of the Tis massif. *Geoscience Research Reports 2003. ČGÚ*, Praha, 13–16 (in Czech).

Breiter K. 2008: Mineral and textural evolution of subvolcanic A-type granite: Hora Svaté Kateřiny stock, Krušné Hory Mts., Czech Republic. *Z. Geol. Wiss.* 36, 365–382.

Breiter K. 2012: Nearly contemporaneous evolution of the A- and S-type fractionated granites in the Krušné hory/Erzgebirge Mts., Central Europe. *Lithos* 151, 105–121.

Breiter K. & Koller F. 1999: Two-mica granites in the central part of the South Bohemian Pluton. *Abh. Geol. B.-A.* 56, 201–212.

Breiter K. & Scharbert S. 1995: The Homolka Magmatic Centre — an Example of Late Variscan Ore Bearing Magmatism in the Southbohemian Batholith (Southern Bohemia, Northern Austria). *Jb. Geol. B.–A.* 138, 9,–25.

Breiter K. & Sulovský P. 2005: Geochronology of the Melechov granite massif. *Geoscience Research Reports 2004. ČGÚ*, Praha, 16–19 (in Czech).

Breiter K., Förster H.-J. & Seltmann R. 1999: Variscan silicic magmatism and related tintungsten mineralization in the Erzgebirge-Slavkovský les metallogenic province. *Mineral. Deposita* 34, 505–521.

Breiter K., Čopjaková R., Gabašová A. & Škoda R. 2005a: Chemistry and mineralogy of orthogneisses in the northeastern part of the Moldanubicum. *J. Czech. Geol. Soc*. 50, 81–94.

Breiter K., Müller A., Leichmann J. & Gabašová A. 2005b: Textural and chemical evolution of a fractionated granitic sytem: the Podlesí stock, Czech Republic. *Lithos* 80, 323–345.

Breiter K., Förster H.-J. & Škoda R. 2006: Extreme P-, Bi-, Nb-, Sc-, U- and F-rich zircon from fractionated perphosphorus granites: The peraluminous Podlesí granite system, Czech Republic. *Lithos* 88,15–34.

Breiter K., Koller F., Scharbert S., Siebel W., Škoda R. & Frank W. 2007a: Two-mica granites of the Plechý (Plockenstein) pluton in the Triple-point area of Austria, the Czech Republic and Germany. *Jb. Geol. B.–A.,* Wien 147, 527–544.

Breiter K., Škoda R. & Uher P. 2007b: Nb-Ta-Ti-W-Sn-oxide minerals as indicator of a peraluminous P- and F-rich granitic system evolution: Podlesí, Czech Republic. *Miner. Petrology* 91, 225–248.

Breiter K., Čopjaková R. & Škoda R. 2009: The involvement of F CO_2–, and As in the alteration of Zr-Th-REE-bearing accessory minerals in the Hora Svaté Kateřiny A-type granite, Czech Republic. *Canad. Mineralogist* 47, 1375–1398.

Cháb J., Breiter K., Fatka O., Hladil J., Kalvoda J., Šimůnek Z., Štorch P., Vašíček Z., Zajíc J. & Zapletal J. 2010: Outline of the geology of the Bohemian Massif. *Czech Geol. Surv.*, Praha, 1–283.

Clarke D.B. 1992: Granitoid rocks. Topics in the Earth Sciences 7. *Chapman & Hall,* 1–283.

Collins W.J., Beams S.D., White A.J.R. & Chappell B.W. 1982: Nature and origin of A-type granites with particular reference so Southern Australia. *Contr. Mineral. Petrology* 80, 89–200.

Cotton F.A. & Wilkinson G. 1980: Advanced inorganic chemistry. *John Wiley*, 1–1396.

Černý P., Goad B.E., Hawthorne F.C. & Chapman R. 1986: Fractionation trends of the Nb- and Ta-bearing oxide minerals in the Greer Lake pegmatitic granite and its pegmatite aureole, southeastern Manitoba. *Amer. Mineralogist* 71, 501–517.

Finch R.J. & Hanchar J.M. 2003: Structure and chemistry of zircon and zircon group minerals. In: Hanchar J.M. & Hoskin P.W.O. (Eds.): Zircon. *Rev. Mineral. Geochem.* 53, 1–26.

Finger F., Roberts M.P., Haunschmid B., Schermaier A. & Steyrer H.P. 1997: Variscan granitoids of central Europe: their typology, potential sources and tectonothermal relations. *Miner. Petrology* 61, 67–96.

Flude S., Burgess R. & McGarvie D.W. 2008: Silicic volcanism at Ljósufjöll, Iceland: insights into evolution and eruptive history from Ar-Ar dating. *J. Volcanol. Geotherm. Res.* 169, 154–175.

Förster H.-J., Trumbull R.B. & Gottesmann B. 1999: Late-collisional granites in the Variscan Erzgebirge, Germany. *J. Petrology* 40, 1613–1645.

Gerdes A., Wörner G. & Finger F. 1998: Late-orogenic magmatism in the Southern Bohemian Massif — geochemical and isotopic constraints on possible sources and magma evolution. *Acta Univ. Carol. Geol.,* Praha 42, 41–45.

Goldschmidt V.M. 1937: The principles of distribution of chemical elements in minerals and rocks. *J. Chem. Soc.*, 655–673.

Goodman R.J. 1972: The distribution of Ga and Rb in coexisting groundmass and phenocryst phases of some basic volcanic rocks. *Geochim. Cosmochim. Acta* 36, 303–317.

Govindaraju K. 1994: Compilation of working values and sample description for 383 geostandards. *Geostandards Newsletter* 18, 1–158.

Hoffmann U., Breitkreutz Ch., Breiter K., Sergeev S., Stanek K. & Tichomirova M. 2013: Carboniferous-Permian volcanic evolution in Central Europe — U/Pb ages of volcanic rocks in saxony (Germany) and northern Bohemia (Czech Republic). *Int. J. Earth Sci.* 102, 1, 73–99.

Holub F.V., Cocherie A. & Rossi P. 1997a: Radiometric dating of granitic rocks from the Central Bohemian Plutonic Complex: constraints on the chronology of thermal and tectonic events along the Barrandian-Moldanubian boundary. *Comptes Rendus de l'Académie de Sciences — Série IIa: Sciences de la Terre et des Planétes* 325, 19–26.

Holub F.V., Machart J. & Manová M. 1997b: The Central Bohemian plutonic complex. *J. Geol. Sci., Econ. Geol., Miner.* 31, 27–49.

Hoskin P.W.O. & Schaltegger U. 2003: The composition of zircon and igneous and metamorphic petrogenesis. In: Hanchar J.M. & Hoskin P.W.O. (Eds.): Zircon. *Rev. Mineral. Geochem.* 53, 27–62.

Höll R., Kling M. & Schroll E. 2007: Metallogenesis of germanium — A review. *Ore Geol. Rev.* 30, 145–180.

Irber W. 1999: The lanthanide tetrad effect and its correlation with K/Rb, Eu/Eu*, Sr/Eu, Y/Ho, and Zr/Hf of evolving peraluminous granite suites. *Geochim. Cosmochim. Acta* 63, 489–508.

Janoušek V. & Skála R. (Eds.) 2011: Bohemian geological enigmas: Variscan high-pressure granulites, ultrapotassic magmatites and tektites. *Goldschmidt 2011 post-conference field trip August 20–22, 2011, Guidebook*, Praha.

Kelly P.J., Kyle P.R., Dunbar N.W. & Sims K.W.W. 2008: Geochemistry and mineralogy of the phonolite lava lake, Erebus volcano, Antarctica: 1972–2004 and comparison with older lavas. *J. Volcanol. Geotherm. Res.* 177, 589–605.

Lenharo S.L.R., Pollard P.J. & Born H. 2003: Petrology and textural evolution of granites associated with tin and rare-metal mineralization at the Pitinga mine, Amazonas, Brazil. *Lithos* 66, 37–61.

Linnen R.L. & Keppler H. 1997: Columbite solubility in granitic melts: Consequences for the enrichment and fractionation of Nb and Ta in the Earth's crust. *Contr. Mineral. Petrology* 128, 213–227.

Macdonald R., Rogers N.W. & Tindle A.G. 2007: Distribution of germanium between phenocrysts and melt in peralkaline rhyolites from the Kenya Rift Valley. *Mineral. Mag.* 71, 703–713.

Macdonald R., Rogers N.W., Baginski B. & Dzierzanowski P. 2010: Distribution of gallium between phenocrysts and melt in peralkaline salic volcanic rocks, Kenya Rift Valley. *Mineral. Mag.* 74, 351–363.

Paktunc A.D. & Cabri L.J. 1995: A proton and electron-microprobe study of gallium, nickel and zinc distribution in chromian spinel. *Lithos* 35, 261–282.

Raimbault L., Cuney M., Azencott C., Duthou J.L. & Joron J.L. 1995: Geochemical evidence for a multistage magmatic genesis of Ta-Sn-Li mineralization in the granite at Beauvoir, French Massif Central. *Econ. Geol*. 90, 548–596.

Shaw D.M. 1957: The geochemistry of gallium, indium, thallium — a review. *Physics and Chemistry of the Earth* 2, 164–211.

Shaw D.M. 2006: Trace elements in magmas. A theoretical treatment. *Cambridge University Press*, 1–243.

Shcherba G.N., Zamyatina G.M., Kalinin S.K. & Mukhlya K.A. 1966: Germanium in some greisens in Kazakhstan. *Geokhimiya* 11, 1365–1368 (in Russian).

Uher P., Breiter K., Klečka M. & Pivec E. 1998: Zircon in highly evolved Hercynian Homolka granite, Moldanubian zone, Czech Republic: indicator of magma source and petrogenesis. *Geol. Carpathica* 49, 151–160.

Venera Z., Schulmann K. & Kröner A. 2000: Intrusion within a transtensional tectonic domain: the Čistá granodiorite (Bohemian Massif) — structure and rheological modelling. *J. Struct. Geol.* 22, 1437–1454.

Vrána S. & Kröner A. 1995: Pb-Pb zircon ages for tourmaline alkali-feldspar orthogneiss from Hluboká nad Vltavou in southern Bohemia. *J. Czech Geol. Soc*. 28, 127–131.

Waldmann L. 1950: Geologische Spezialkarte der Republik Österreich 1:75,000, Blatt Litschau-Gmünd (4454). *Geologische Bundesanstalt*, Wien.

Wedepohl K.W. 1972: Handbook of geochemistry. *Springer*, part 2, vol. 3, 1–900.

Whalen J.B., Currie K.L. & Chappell B.W. 1987: A-type granites: geochemical characteristic. Discrimination and petrogenesis. *Contr. Mineral. Petrology* 9, 407–419.

Contents of SiO_2, Al_2O_3, and K_2O (wt. %) and Ge, Ga, Rb, Y, and Ho (ppm) in analyzed samples								
No.	**SiO_2**	**Al_2O_3**	**K_2O**	**Ge**	**Ga**	**Rb**	**Y**	**Ho**
Moldanubicum orthogneisses								
4080	70.1	15.8	3.20	1.3	22.6	142	11	0.35
4069	70.8	15.0	4.41	1.7	18.3	217	25	0.80
4066	70.5	14.8	5.02	1.7	19.8	260	34	1.18
4072	72.9	13.5	5.24	1.6	19.8	391	37	1.24
4074	72.9	14.6	4.91	3.2	20.9	369	15	0.45
3266	74.0	14.5	4.38	2.7	20.9	329	10	0.30
3796	72.8	14.6	4.51	2.7	19.1	269	11	0.38
3262	74.7	14.6	3.89	4.3	27.9	573	4.0	0.11
Tis Pluton								
3315	65.7	14.7	3.30	1.48	19.1	92	61	2.10
4658	72.9	13.3	2.88	1.5	20	80	52	1.86
3230	73.9	13.3	4.58	1.3	18	133	37	1.25
3231	73.7	13.1	4.54	1.44	18.3	149	22	0.74
4653	67.5	14.9	4.28	1.9	20.8	141	33	1.12
Central Bohemian Pluton								
4848	74.0	13.8	2.48	1.5	14.3	70	11	0.33
4849	63.6	18.8	2.32	1.6	16.8	63	7	0.23
4845	65.5	15.2	3.81	1.7	19.8	182	17	0.58
4846	63.0	15.5	3.63	1.8	21.6	171	25	0.97
4847	66.0	14.4	5.47	2.1	21.1	318	22	0.79
4850	69.0	15.8	5.57	2.1	24.7	329	10.4	0.36
South Bohemian Pluton								
4084	71.3	15.2	5.39	1.8	24.8	347	9.2	0.28
4231	70.0	14.8	5.36	1.7	24.5	321	17	0.49
2793	72.0	14.7	5.14	1.5	22.0	295	9.4	0.30
4265	71.4	15.3	5.35	1.0	21.2	328	10.6	0.35
4089	72.0	15.6	4.42	2.2	20.4	299	10.8	0.36
4093	71.5	15.9	4.58	2.2	21.7	308	11.3	0.40
2772	72.7	14.9	3.18	1.3	22.4	140	5.9	0.20
2761	73.9	14.3	4.60	1.8	16.6	252	7.9	0.26
2771	75.1	13.8	4.28	1.6	18.7	232	12	0.38
2782	72.1	14.8	5.33	1.6	22.1	289	7.8	0.22
3024	73.4	14.1	5.39	1.3	24.1	284	7.3	0.24
2774	74.3	13.7	4.27	1.7	23.9	291	10.0	0.33
2944	70.7	14.9	5.41	1.5	26.3	284	10.0	0.33
2962	73.9	14.3	4.60	1.6	25.9	252	7.9	0.26
3009	73.2	14.3	5.19	1.8	23.7	306	8.3	0.28
2777	72.9	14.4	4.66	1.7	22.4	290	9.9	0.33
2940	72.4	14.3	4.79	1.8	22.8	283	8.9	0.27
2949	71.3	15.0	5.91	1.8	25.3	382	7.4	0.23
2954	73.6	14.1	4.60	2.3	27.3	402	10.3	0.31
2964	71.3	14.6	5.12	2.8	26.8	335	10.4	0.31
2511	73.6	14.8	3.83	4.2	29.1	734	5.7	0.17
2512	72.8	15.1	3.23	5.4	26.4	1023	1.7	0.05
2513	73.4	15.5	3.14	4.0	29.8	1188	1.2	0.03
2476	73.4	14.3	2.39	5.5	33.1	574	1.6	0.05
2513	74.3	14.5	3.14	6.2	31.0	1188	1.2	0.03
4139	71.5	14.2	5.53	1.7	29.4	420	15	0.44
4362	71.8	14.5	5.21	1.4	27.6	405	17	0.54
4368	73.6	14.4	5.32	1.6	21.3	348	9.0	0.30
3612	73.2	14.9	4.85	1.9	24.3	374	11	0.31
4363	73.2	14.0	5.26	1.7	33.0	423	14	0.47
4365	72.4	14.3	4.99	1.6	23.7	457	14	0.43
Nejdek Pluton								
2924	72.4	13.9	4.71	2.2	20.1	240	16	0.52
2925	72.4	14.4	4.80	2.0	21.7	260	17	0.54
4742	71.5	14.2	4.36	1.5	22.5	227	19	0.64
4743	72.1	14.7	4.58	1.3	22.4	250	16	0.51
4744	74.8	13.3	5.02	1.2	27	416	21	0.67
4745	72.5	15.0	4.62	2.8	35	978	13	0.39
Podlesí stock								
3475	73.6	14.3	4.50	3.6	37.2	1212	9.6	0.26
3490	73.8	14.6	4.21	5.0	37.5	1502	6.8	0.18
3385	73.8	14.6	4.46	3.4	32.5	1229	11	0.27
3458	73.2	14.8	4.07	3.6	36.2	1316	6.7	0.20
3464	73.7	14.4	4.28	3.6	33.9	1186	8.7	0.24
3511	72.6	14.8	4.15	4.1	34.4	1270	7.4	0.19
3413	72.5	16.0	3.51	3.9	52.6	2010	2.3	0.03
3414	70.7	15.9	3.80	4.4	54.5	2165	1.5	0.02
3416	70.1	15.8	4.25	3.9	69.3	2021	2.2	0.04
3417	66.5	17.8	6.42	4.4	77.4	2754	2.8	0.05
3366	77.6	14.9	0.46	8.8	10.9	370	11	0.29
3387	81.8	13.2	0.32	7.6	7.8	87	12	0.36
Hora svaté Kateřiny								
4471	76.6	12.2	5.56	2.5	31.7	390	36	1.44
4604	77.1	12.6	4.62	3.1	40.1	606	40	1.39
3097	74.2	13.2	4.58	3.7	38.3	1067	157	3.55
4554	75.5	12.6	4.36	3.4	37.7	1147	111	2.31
Teplice caldera								
3194	76.1	12.3	5.13	1.6	20.9	393	60	1.97
3198	74.7	12.3	5.61	1.4	19.9	475	76	2.60
3201	76.4	12.3	5.42	1.1	18.1	246	36	1.26
3207	77.1	11.6	4.66	2.3	24.4	394	67	2.36
3208	76.4	11.8	6.32	1.4	20.3	248	21	0.80
3210	75.8	12.2	4.97	1.9	21.2	399	44	1.41
3211	61.4	24.4	0.91	2.3	32.4	59	30	0.98
3532	68.9	14.7	5.70	1.9	23.9	208	38	1.24
3376	68.1	14.7	5.88	1.7	23.7	182	36	1.25
4686	75.9	13.6	13.57	2.9	47	1393	21	1.06
4687	75.8	12.5	12.52	3	40	1390	131	4.38
4691	75.6	12.8	12.76	2.8	35	1133	114	3.94
4692	75.4	12.5	12.46	1.5	28.9	724	108	3.41
4693	75.5	12.6	12.55	1.7	32.4	802	103	3.44